Modelling Chug Instabilities by Variable Time Lag Approach

Marco Leonardi*[1], Francesco Di Matteo†[2], Johan Steelant‡[2], Francesco Nasuti§[1], and Marcello Onofri¶[1]

[1]*University of Rome "La Sapienza", Dip. Ingegneria Meccanica e Aerospaziale, Rome, Italy*
[2]*ESA-ESTEC, Aerothermodynamic & Propulsion Analysis Section, Noordwijk, The Netherlands*

Abstract

In this paper we propose an analysis of low frequency combustion instabilities, taking advantage of the software EcosimPro. We implement a specific module based on the double time lag model and investigate the coupling of combustion chamber and feed line oscillations by using a complete set of non-linear equations. We identify the characteristic time lags following two approaches: (i) a constant time lag approach and (ii) a variable time lag approach based on correlations available in open literature. To prove the module capabilities we reproduce an experimental set up consisting of a combustion chamber decoupled from the upstream feed lines. For this configuration we generate a stability map, comparing our results with literature data from both experiments and a linear double time lag model. The stability boundaries obtained with the chug module are in good agreement with those obtained in open literature, and the first characteristic frequency of the engine is well predicted. Finally, we study the influence of the feed lines on the system stability, verifying that the lines extend the stable regime of the combustion chamber and that the propellant domes play a key role in coupling the dynamics of combustion chamber and feed lines.

NOMENCLATURE

Δp	Injector pressure drop
ρ	density
ξ	pressure drop coefficient
A	cross section area
E	total energy
H	total enthalpy
MR	mixture ratio
p	pressure
R	gas constant
T	temperature
t	time
u	velocity
V	volume
x	axial coordinate

Subscripts

$atom$	atomisation
c	chamber
$crit$	critical conditions
fu	fuel
g	gas
l	liquid
ox	oxidizer
th	throat
vap	vaporisation

*Ph.D, marco.leonardi@uniroma1.it
†Ph.D, Propulsion Engineer, francesco.di.matteo@esa.int
‡Ph.D, Propulsion and Aerothermodynamic Engineer, johan.steelant@esa.int
§Associate Professor, francesco.nasuti@uniroma1.it
¶Full Professor, marcello.onofri@uniroma1.it

1 Introduction

In this paper we propose an analysis of low frequency combustion instabilities, frequently referred to as chugging, where the typical components of a Liquid Rocket Engine (LRE) are modelled with an unsteady non-linear approach. Low frequency combustion instabilities in liquid rocket engines are characterised by oscillations in the mass flow rate of propellants that result in pulsations of the chamber pressure. The response of the combustion chamber to the upstream oscillations is not immediate. The delay is due to the different characteristic times associated with the processes of injection, atomisation, vaporisation, mixing and combustion, taking place in quick succession inside the combustion chamber. Moreover, the mass flow rate is not immediately responsive to pressure oscillations, because of the propellant inertia in the feed lines. Hence, both feed lines and combustion chamber physics must be taken into account. Low frequency instabilities have been usually investigated with the help of linearised models [1, 2, 3, 4, 5], whereas only a few attempts have been made to detail the phenomena with non-linear models [6, 7]. In the present study we propose an unsteady non-linear analysis of chug instabilities, with particular attention to the appropriate modelling of delays induced by atomisation, vaporisation and mixing processes.

The analysis of chug instabilities requires to model the subsystems of a LRE to investigate the mutual influence of each component. Such a comprehensive simulation inherently needs simplified sub-models able to give a satisfactory level of

reliability along with a reasonable computational time. In this context an object oriented simulation tool is a valid option to handle the complexity of a propulsion system. EcosimPro [8] is a simulation platform focused on the analysis of complete systems that spans different engineering fields. Thanks to the object oriented philosophy single components can be connected to each other in order to analyse systems at different complexity levels. Propulsion systems can be investigated by the European Space Propulsion System Simulation (ESPSS) library [9], in which the typical components of a liquid rocket engine (tanks, turbo machinery, feed lines, valves, gas generator/pre-burner, combustion chamber, etc.) are modelled to study both steady state and transient phases.

To detect low frequency instabilities it is important to properly model the characteristic times associated with both liquid and gases injected into the combustion chamber. Chug instabilities arise when the total time lag is such that oscillations in the rate of propellant injection are coupled with the corresponding oscillations of the chamber pressure. Different studies have been performed during the past decades to investigate which time lag is the most important for the generation of low frequency instabilities. Most of the proposed chug models focused on steady linear analyses based on the linearisation of the continuity equation in the combustion chamber. In the attempt of explaining damages caused by chugging in LRE, Gunder and Friant [3] introduced the time lag concept. They linearised the energy conservation equation and solved the relative delay differential equation. The time lag approach was then further extended by Summerfield [2], that retrieved a stability analysis from the linearisation of the continuity equation introducing the influence of the feed lines. He investigated the effects of feed lines, injector pressure drops and combustion chamber length on chug instabilities. A comprehensive theoretical approach based on the concept of sensitive and in-sensitive time lag was then proposed by Crocco and Cheng [5, 10, 11]. Their approach is based on the concentrated combustion model and applies to both mono-propellant and bi-propellant cases. Later, Wenzel and Szuch [4, 12, 13, 14] developed a model that incorporates a double time lag approach, hence extending the potentialities of the original Crocco's model to cases in which the two propellants have different time lags. They applied the model to analyse a system ignoring the influence of the feed lines and considering only the injector impedances. They used a useful engineering approach to express the solutions, highlighting the importance of injector pressure drops on instabilities. Recently, Casiano [1] extended the Wenzel and Szuch's model by formulating the problem in a parametric form and adding the influence of the feed lines. Linear models have been also developed to study Pogo instabilities, that are combustion instabilities characterized by the coupling of combustion and structural dynamics and that usually brings to structural as well as thrust oscillations. Pogo instabilities arise at low frequencies well below 100 Hz, thus making Pogo models appealing for the study of chug instabilities. Such is the case of Ordonneau's work, where a Pogo model, originally meant to study Pogo instabilities in the VULCAIN engine, has been adapted to both analyse chug instabilities of VULCAIN and predict those of VULCAIN 2 engine [15, 16]. Beside these linear approaches a few attempts have been made in the field of non-linear analysis, mainly because the computational cost of such approaches was too high for the hardware resources. Webber's [6] work was the first attempt of performing an unsteady analysis based on non-linear equation for both the feed lines and the combustion chamber. He focused his attention towards the modelling of the liquid phase in the combustion chamber, showing the effects of droplet sizes on the amplitude of the low frequency oscillations. Bartrand [7] proposed an extension of this model, including the effects of finite rate chemistry and showed that, in the Space Shuttle Main Engine pre-burner case, the assumption of finite combustion velocity affects the magnitude of the damping rather that the frequency of oscillations.

The analyses conducted in this paper take advantage of the ESPSS feed lines modelling approach, whereas the combustion chamber component is suitably improved by means of a chug dedicated module. It is well known that the shift, or time lag, between disturbances coming from injectors and pressure response is the sum of five time lags [17], each related to a specific process taking place in the combustion chamber. The five processes are, in order: injector response, atomisation, vaporisation, mixing, combustion. It is commonly accepted that the most important delays are those related with atomisation, vaporisation and mixing [18, 7], whereas spatial droplet distribution produced by injection has been shown to have a great effect on high frequency instabilities but has a little or no effect on chugging [13]. Moreover, combustion processes are usually considered as infinitely fast. On the contrary, the vaporisation rate is of great importance for the evaluation of chugging and is strictly related with the atomisation process (droplet size and surface area). Therefore, we focus our attention on atomisation, vaporisation and mixing phenomena. Two different approaches are foreseen: a constant time lag approach and a variable time lag approach. In the constant time lag approach atomisation, vaporisation and mixing time lag remains unchanged throughout the entire simulation. Instead, for the variable time lag approach both atomisation [19] and vaporisation [19, 20] will be modelled with the aim of semi-empirical correlations while mixing times will be retrieved from an empirical curve [12]. In this way the characteristic times depend on the main combustion chamber parameters, thus changing during the simulation. The chug module reliability with the two approaches will be proved by comparisons against experimental and numerical data available in open literature [21]. Finally, the influence of the feed lines on the stability of the engine will be studied by means of specific parametric analyses on the most important system parameters (e.g. injector pressure drops and dome volumes).

2 Numerical Method and Approach

The LRE system is here modelled with EcosimPro, taking advantage of the components included in the European Space Propulsion System Simulation (ESPSS) library, for which a complete description can be found in the different works [9, 22]. In the following the feed lines and injector components are briefly introduced whereas more details are provided for the combustion chamber component. The modelling approach for the gas phase in the combustion chamber is particularly important for the scope of the present paper, because it is the frame in which the vaporisation, atomization and mixing models are included.

2.1 System Components

2.1.1 Feed Line and Injector Components

The tube component is modelled with a quasi-one-dimensional, unsteady approach for two phase flow. The two phase flow evolution is described by the Homogeneous Equilibrium Model [23] (HEM), which is based on the assumptions: (i) thermodynamic equilibrium between the two phases, (ii) same velocity for both liquid and vapour. Hence, two mass conservation equations are foreseen, one for the total mass and one for the vapour phase, completed by a momentum and an energy equation. This approach has the advantage to be governed by a set of equations that is unconditionally hyperbolic, hence allowing the use of widespread techniques for the calculation of the interface fluxes.

Injectors and injector cavities are located between the feed lines and the combustion chamber. Injector cavities are modelled by means of a two-phase set of equations for a non adiabatic variable volume. Two mass conservation equations and one energy equation describe the evolution of the two-phase mixture. The velocity in the cavity is calculated as an average velocity retrieved from the mass flow rate of the incoming fluid (calculated by the tube component) and the fluid going to the combustion chamber (calculated by the injector component), hence no momentum equation is solved. Finally, the injector component is based on a momentum equation to derive the mass flow across the injector in both turbulent and laminar regimes. The momentum equation accounts for concentrated pressure losses and for the inertia associated with the connected components. In this way both mass and energy fluxes are provided to the combustion chamber component.

2.1.2 Combustion Chamber

The thrust chamber component consists of two sub-components. The first one is an unsteady component that simulates the combustion chamber up to the throat. In this part of the combustion chamber the flow is considered either in chemical equilibrium or in a "time delayed" equilibrium state. In the present analyses we will consider the component as based on the chemical equilibrium assumption. Instead, the divergent part is a quasi-steady component that mimics the supersonic expansion by means of analytical correlations for a flow in either frozen or equilibrium conditions.

The first part of the combustion chamber is based on a quasi-one-dimensional formulation of the governing equations. The component is non adiabatic, hence allowing for thermal connections with the external components, i.e. cooling channels. The unsteady conservation equations for the gas mixture are:

Mass

$$A\frac{\partial \rho}{\partial t} + \frac{\partial(\rho u A)}{\partial x} = \frac{A\,\dot{m}_{vap}}{V} \tag{1}$$

Momentum

$$A\frac{\partial(\rho u)}{\partial t} + \frac{\partial[(\rho u^2 + p)A]}{\partial x} = -\frac{1}{2}\frac{d\xi}{dx}\rho u\,|u|\,A + p\left(\frac{dA}{dx}\right) \tag{2}$$

Energy

$$A\frac{\partial(\rho E)}{\partial t} + \frac{\partial(\rho u H A)}{\partial x} = \frac{\delta \dot{q}_w}{dx} + \frac{\delta \dot{q}_{unst}}{dx} + \dot{m}_{vap}\Delta q_{vap} \tag{3}$$

The first source term on the right hand side of the momentum equation models the friction effects, while the second is related to the effects of a variable area. The first source term in the energy equation $\dot{q}_w$ is the heat exchanged with the combustion chamber walls while the second term $\dot{q}_{unst}$ is the unsteady heat release introduced in the present analysis to mimic the roughness of the combustion processes. Finally, the vaporised mass source term in the continuity equation $\dot{m}_{vap}$ is expressed according to the vaporisation models described in the next section.

The nozzle component is a quasi-steady component able to describe the evolution of a flow in a duct with variable cross section. The nozzle takes the upstream thermodynamic state from the last computational cell of the combustion chamber and characterises the throat and the diverging section conditions. It should be noted that the modelling of the supersonic evolution is not directly needed to properly model chug instabilities since the only boundary condition that affects the detection of chug instabilities is the one giving the mass flow evolution at the throat section. However, we leave the component in its original formulation as the presence of the diverging nozzle does not limit the chug model capabilities.

2.1.3 Time Lag Approach

Once injected into the combustion chamber the liquid subsequently undergoes atomisation, vaporisation, mixing and combustion. The time lags of each process must hence be characterised in an appropriate way in order to catch the coupling between the feed lines and the combustion chamber. The general numerical procedure is the following: once injected in the combustion chamber the mass associated with the liquid droplet is stored in a memory array and conserved

for a time equal to the total time lag (vaporisation, atomisation and mixing) associated with the droplet. After the ascribed time lag the incoming mass is injected as a vaporised source term in the gas conservation equation (1). Two different cases are foreseen. A first one in which the time lags are user-defined input parameters and remain constant throughout the simulation. The second case is instead based on a time delayed approach in which the vaporisation and atomisation processes are described by time lags based on chamber conditions and liquid phase characteristics. The mixing times are retrieved from an empirical curve [12], while the combustion is considered as sufficiently fast and its time lag can be neglected. In the present study we decided to focus our attention towards the oxygen-hydrogen combination, hence the correlations applied to the characteristic times hold only for these propellants. In particular the hydrogen is injected in a gaseous phase, therefore the delay characterising this propellant is only the mixing time lag. The oxidizer is instead injected in a liquid phase, hence it experiences also vaporisation and atomisation. The time lags and the related parameters are calculated as follows. For the atomisation processes we apply the correlation [19]:

$$\tau_{atom} = 6 \cdot 10^{-4} \cdot \left(\frac{\rho_g}{\rho_l}\right)^{-0.32} We_g^{0.03} Re_l^{0.55} \frac{D_l}{u_l} \tag{4}$$

$$Re_l = \frac{u_l D_l \rho_l}{\mu_l} \quad We_g = 2\rho_g \frac{(u_g - u_l)^2 D_l}{\sigma_l} \tag{5}$$

where D_l is the liquid post inner diameter (m), u_l is the liquid velocity at injection (m/s), σ_l the liquid surface tension (N/m), Re_l the Reynold's number for the injected droplet and We_g the Weber number for the combustion chamber gases.

Vaporisation characteristic times for droplets when in presence of convection [24, 25, 19, 26] are usually retrieved as a correction of those obtained for droplets immersed in a quiescent gaseous environment [27]. We here make use of the correlation [19]:

$$\tau_{vap} = \frac{\tau_{vap,Re=0}}{1 + 1.5\alpha} \qquad \alpha = 1 - \frac{0.3 p_c}{100} \tag{6}$$

$$\tau_{vap,Re=0} = \frac{D_0^2}{k} \tag{7}$$

$$k = 10^{-6} \left[1.01 \frac{1}{1+MR} + 1.16 \cdot 10^{-3} (T_\infty - T_{cr})^{0.93}\right]^{0.86} \tag{8}$$

where p_c is the chamber pressure (bar), MR the mixture ratio, T_∞ the temperature of the combustion chamber gases (K), T_{cr} the liquid critical temperature (K) and D_0 the initial droplet diameter (m). The initial droplet diameter D_0 is here calculated from a correlation specifically developed for coaxial injectors and liquid oxygen [20]:

$$D_0 = C_{inj}\ K\ 127 \left(\frac{V_r}{160}\right)^{-0.93} \left(\frac{D_l}{2}\right)^{2.25} \cdot \left(\frac{D_g}{3}\right)^{-2.65} \left(\frac{R_{post}}{D_l}\right)^{-0.26} \tag{9}$$

D_c	chamber diameter [cm]	5.08
D_{th}	throat diameter [cm]	1.24
L^*	characteristic length [m]	2.31
L_c	chamber length [cm]	10.4
MR	mixture ratio [-]	5
p_c	chamber pressure [bar]	44.8
$\dot{m}_{ox}$	mass flow rate [kg/s]	0.249
$V_{cav,ox}$	oxidizer injector cavity volume [m^3]	1e-5
$V_{cav,fu}$	fuel injector cavity volume [m^3]	1e-5

Table 1: Main engine parameters

Component	Description
LOX/GH2	Propellant definitions
BC_ LOX/LH2	Boundary conditions for propellant lines
MOV	Main Oxidizer Valve
MFV	Main Fuel Valve
Heater_ 1	Heat source
Loss	Heat losses time law
Insulation_ 1	Thermal insulation (zero heat flux)
SZC_ CHUG	Combustion chamber

Table 2: EcoosimPro component descriptions of Figure 1

being V_r the relative velocity between injected liquid and gases in the combustion chamber (m/s), D_g the annular gap outer diameter (m), R_{post} the recess length (m), C_{inj} a parameter taking into account the injector design ranging from 0.4 to 1.2 and K a correction factor to be applied when the experimental simulants differ from the actual propellants [28].

3 Test Case

In order to prove our chug module capabilities we refer to an experimental test case specifically developed to validate a linear double time lag model [21]. The experimental apparatus is a gaseous-hydrogen liquid-oxygen engine. The injector cavities and injector plate were specifically designed to ensure the desired pressure drops and a constant pressure in the injector cavities. The main engine parameters are described in Table 1, while the EcosimPro schematic and its component descriptions are proposed respectively in Fig. 1 and in Table 2.

Following the approach proposed in the reference work [21], we define a stability map for the engine by performing simulations with variable injector pressure drops. Changing both fuel and oxidizer pressure drops it is possible to create a map in which stable and unstable regions can be identified. The combustion inside the chamber is a rough process, hence spontaneous oscillations in the pressure values are usually experienced. In order to mimic these oscillations and trigger the instabilities we decided to introduce an unsteady term in the energy equation. The purpose is here to reproduce

the unsteady heat release associated with combustion, phenomena commonly identified as the triggering mechanism for combustion instabilities. The unsteady heat release term is represented by means of a broadband signal. The broadband reported in eq.(10) precisely selects the frequencies of interest and, in the hypothesis of small perturbations, enables the analysis of the chamber response at the selected frequencies

$$\dot{q}_{unst} = \dot{q}_0 \cdot \left[1 + \epsilon \sum_{i=1}^{N} sin(2\pi(f_0 + i\Delta f)t)\right] \qquad (10)$$

being f_0, Δf, N, ϵ respectively the first excited frequency, the sampling frequency, the number of samples and the magnitude of the perturbation. In this way frequencies between f_0 and $f_0 + N\Delta f$ are excited every Δf. The steady value $\dot{q}_0$ is selected to mimic the losses measured in the combustion facility in order to match the experimental combustion efficiency $\eta_{c^*} = 0.75$. The value is kept constant throughout all the simulations and equal to $\dot{q}_o = 1.933$ MW. This gives a low value of the combustion chamber temperature $T_c = 2038$ K, as expected from the low combustion efficiency.

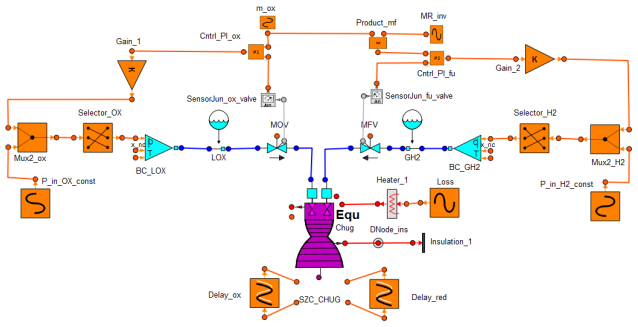

Figure 1: System schematic for chug analysis: combustion chamber without feed lines

Pressure boundary conditions on both feed lines are changed throughout the simulations to ensure constant mass flow rates at steady state for different injectors pressure drops. It is worth saying that EcosimPro has its own component to ensure a constant mass flow rate in the feed line. This component could have been replaced in the schematic in Fig. 1 both main oxidizer and main fuel valves, thus imposing the desired mass flow rates. However, it has been verified that the use of this component adds an artificial damping preventing the system from falling in any instability regime, hence failing in detecting chugging.

4 Results

4.1 Combustion Chamber

4.1.1 Constant Time Lag

In the case of constant time lag the characteristic times are imposed as user input data. The values here used are inferred from the reference work [21]. In particular, the atomisation time is in this case neglected and the vaporisation lag is retrieved from the length needed to vaporise the 50 percent of the injected liquid mass l_{50} [29]. Once the length is known the vaporisation time is calculated as the ratio of the vaporisation length and the injection velocity of the liquid, $\tau_{vap} = l_{50}/v_{inj}$. Calculations for the examined engine configuration give a value of $\tau_{vap} = 4.4$ ms. The mixing and reaction times are then retrieved from the neutral stability condition. Starting from the experimentally observed chug frequency at high injector pressure drops of 68 Hz, the phase requirement for stability gives an overall time delay of $\tau_{tot} = 6.7$ ms. Hence, the mixing time lag is obtained as a difference of the previously calculated delays $\tau_{mix} = 2.23$ ms.

The results obtained with the chug module are here compared to those coming from both experimental evidences and Szuch's double time lag model. The tests are performed by assigning one of the two injector pressure drops, varying the other and measuring the response in terms of chamber pressure. The Root Mean Square (RMS) of the oscillations of the measured signal is then extracted and presented in terms of percentage values with respect to the mean chamber pressure, while the frequency content is analysed by means of the signal Power Spectral Density (PSD). In this way we are able to retrieve both amplitude of the response and characteristic frequency of the system. It is worth noticing that the amplitude of the chamber response is strictly related to the amplitude of the input perturbation, that in turn affects the definition of the stability region. In the experimental campaign here referenced [21] a 10 percent RMS criterion was used to identify stable and unstable operating regimes. In particular, all the configurations that give a pressure signal with a RMS exceeding the 10 percent of the mean chamber pressure value are considered unstable, while all the others can be considered stable. The same consideration applies to the results coming from the simulation performed by Szuch and Wenzel for, where they imposed a white noise signal on the mean combustion products values to mimic the roughness of the combustion processes. The white noise input perturbation affects the entire spectrum but we are just interested in the lower part of the spectrum, since chug instabilities are associated with low frequencies. This consideration justifies our choice of a broadband input. In the subsequent analysis the broadband signal is characterised by the values $f_0 = 0$ Hz, $\Delta f = 5$ Hz,$N = 20$ and $\epsilon = 0.01$, with reference to eq.(10). In Fig. 2 we compare results obtained with the chug module for both single and double time lag cases against those presented by Szuch and Wenzel for both analog and exper-

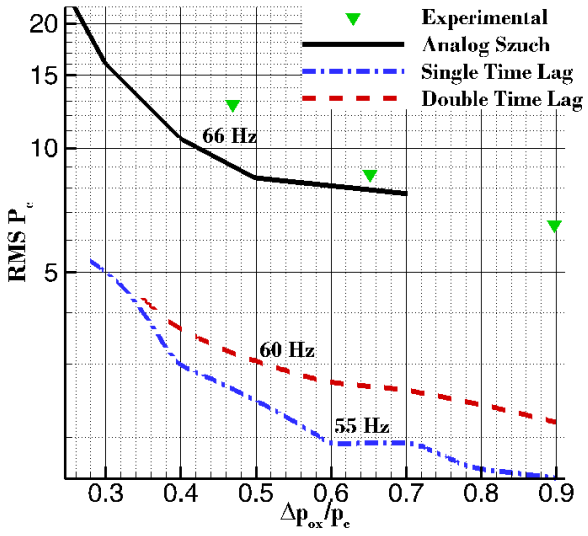

Figure 2: Double vs. single time lag, $\Delta p_{fu}/p_c$ = 0.5: percentage chamber pressure RMS vs oxidizer injector pressure drops: Szuch's experimental and numerical approach vs Ecosimpro

imental cases. In the single time lag case only the injected liquid droplets are included in the chug module and are introduced with a time lag equal to the sum of vaporisation, atomisation and mixing delays into the continuity equation. In the double time lag case a delay equal to the mixing time lag is imposed also to the injected gaseous fuel. Results are obtained imposing a constant fuel injector pressure drop of $\Delta p_f/p_c = 0.5$, varying the oxidizer injector pressure drops and measuring the pressure response at different points. Both of our methods (single and double time lag) are able to catch the increase in the RMS pressure values associated with the reduction of pressure drops. This is a well known behaviour since increasing the injector pressure drops has a stabilising effect on the overall system and decouples the oscillations in the feed lines of liquid oxygen from those in the combustion chamber, thus preventing the system from falling in the unstable regime. The predominant frequency resulting from the PSD in the single time lag case (55 Hz) differs from the one of the double time lag case (60 Hz). The result of this prediction has to be discussed considering that the broadband sampling frequency Δf introduces an uncertainty of ± 5 Hz. The difference between the two approaches is related to the fact that in the double time lag also the fuel feed line couples dynamically with the oscillations in the combustion chamber, thus changing the phase relation between lines and combustion chamber. However, the small registered shift indicates that the chug frequency is mostly determined by the liquid oxygen, since the greater time lag is associated to this propellant and it dominates the phase relation between oscillations. Furthermore, in the single time lag case the RMS values are always smaller than those of the double time lag approach and a plateau is observed between $\Delta p_f/p_c = 0.6$ and $\Delta p_f/p_c = 0.7$. Furthermore, both the time lag approaches give a RMS values of the chamber pressure that are lower than those registered in the reference test cases. This is related with the amplitude ϵ of the broadband in eq.(10). In Fig. 3 we show the influ-

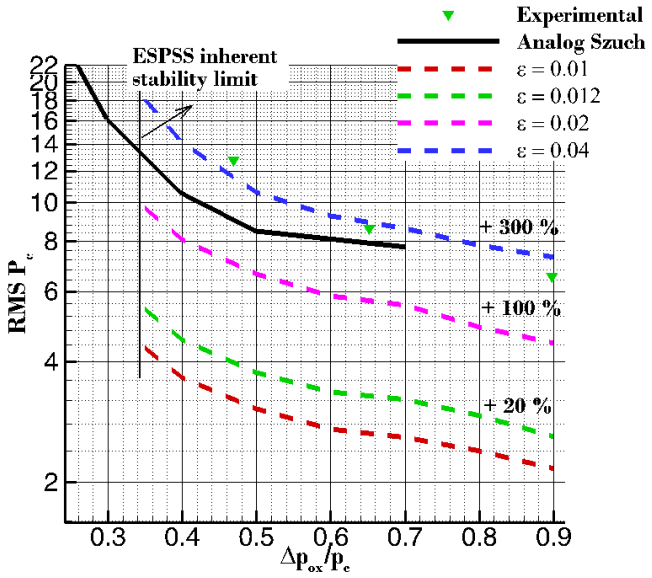

Figure 3: Double time lag, $\Delta p_{fu}/p_c$ = 0.5: percentage chamber pressure RMS vs oxidizer injector pressure drops at different input amplitudes

ence of the amplitude of the broadband signal on the chamber pressure. Increasing the amplitude of the input perturbation increases the chamber pressure response and the values reported in the reference paper are approached. It must be noted that in our double time lag model the inherent stability limit is placed before the one proposed in the reference work, and this is true for all the selected level of amplitudes. In both single and double time lag approaches the system response to the broadband can be divided in three zones characterised by a different behaviour in terms of both frequency content and signal shape. In Fig. 4 and Fig. 5 we show respectively the time evolution of chamber pressure and the PSD of the same variable in the case the double time lag model. Similar trends have been noted in the single time lag case. At high oxidizer pressure drops the chamber pressure signal is proportional to the input signal, with a frequency content characterised by a small peak at 60 Hz. When the oxidizer injector pressure drop is reduced, the 60 Hz frequency becomes predominant and the pressure signal assumes a characteristic damped behaviour. At $\Delta p_f/p_c = 0.35$ the system is still able to damp the perturbation and to prevent the oscillations from growing. No limit cycle is observed and the chamber pressure oscillations are damped and tend to disappear if not sustained with the input broadband signal. Below the inherent stability limit, $\Delta p_{ox}/p_c < 0.35$ the system is not able to damp the oscillations and the pressure response grows to high values causing the simulation to fail, as shown in Fig. 4(d). In

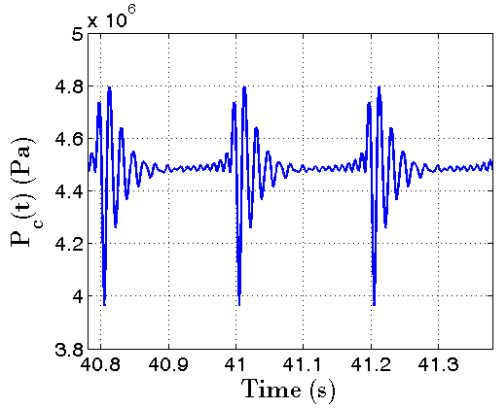

(a) $\Delta p_{ox}/p_c = 0.5$

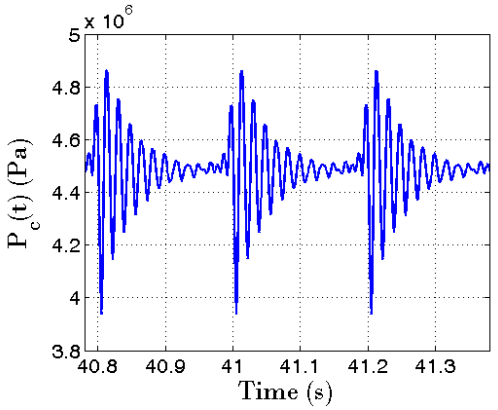

(b) $\Delta p_{ox}/p_c = 0.4$

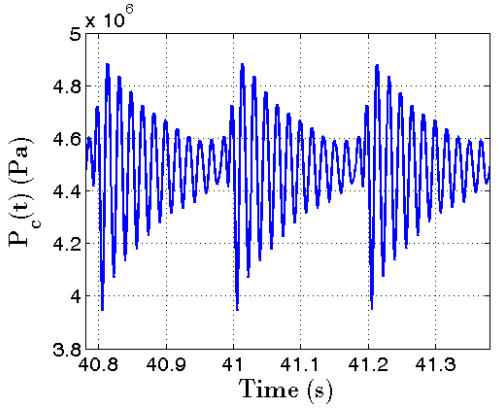

(c) $\Delta p_{ox}/p_c = 0.35$

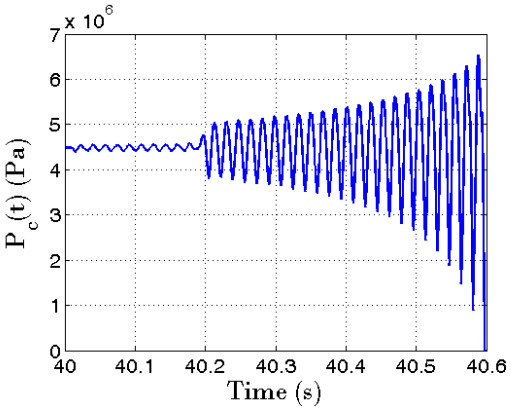

(d) $\Delta p_{ox}/p_c = 0.3$, undamped case

Figure 4: Double time lag, $\Delta p_{fu}/p_c = 0.5$: Time evolution of the chamber pressure response at different oxidizer injector pressure drops

this case the system oscillates at the system characteristic frequency of 60 Hz and the oscillations are self sustained even when the input is turned off. Furthermore, the system oscillates at the characteristic frequency regardless the frequency content of the input, that is: the system diverges with a 60 Hz frequency even if a monochromatic input of 20 Hz is imposed for a short time and then deactivated. In Fig. 6 we propose the stability map obtained for the selected test case with the double time lag model. The results are compared with the boundaries identified by Szuch and Wenzel It is worth noticing that the 10% RMS criterion is a practical criterion [21] to define a stability boundary. Since this criterion is directly related with the amplitude of the input perturbation we choose to use a value of $\epsilon = 0.01$ throughout the simulations and we make use of also a 50% RMS criterion to identify the stability boundary. The stability identified with both the 10% and the 50% RMS criterion are shown with white dashed lines, whereas the reference results are shown in black. When the boundary is identified with the 50% criterion the reversal in slope at lower $\Delta p_f/p_c$ is well matched, and, differently from the analog referenced computer program, no unstable regimes are identified at high oxidizer injector pressure drops when the fuel injector pressure drop is lower than 0.15. The authors of the reference paper [21] justified this discrepancy assuming a back-flow in the fuel injector element at lower pressure drops, however this back-flow has never been registered in our simulations. Furthermore, the reversal in slope is due to the intersection of two boundaries: the low frequency boundary and the high frequency boundary. At lower fuel injector pressure drops characteristic system frequencies ranging from 147 to 210 Hz were observed both experimentally and numerically [21]. In order to investigate the presence of this second frequency we extend the broadband input up to 200 Hz, measuring the resulting chamber pressure signal. With this input we are able to register a higher frequency content of 175 Hz that is well within the limits of the aforementioned high frequency range, giving a ratio of 2.9 between higher and lower frequency that well approximates the 2.7 ratio noted during multi-mode oscillations [30]. However, when the system enters its unstable regime at fuel injector pressure drops lower than 0.15 the pressure diverges with a frequency of 60 Hz, thus meaning that in our analysis the 60 Hz frequency is the characteristic frequency of the system even at lower fuel injector pressure drops. Furthermore, the PSD shows that the power associated to the 60 Hz component is always greater than the one at 175 Hz, explaining the predominance of the first frequency throughout the entire stability map.

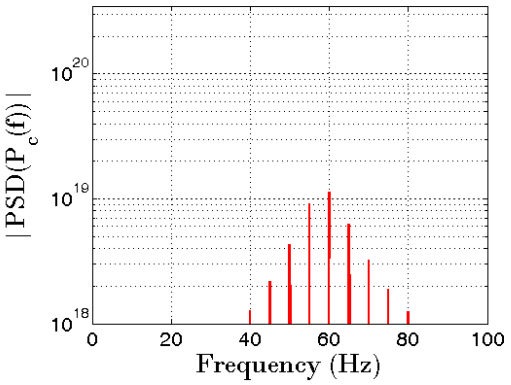

(a) $\Delta p_{ox}/p_c = 0.5$

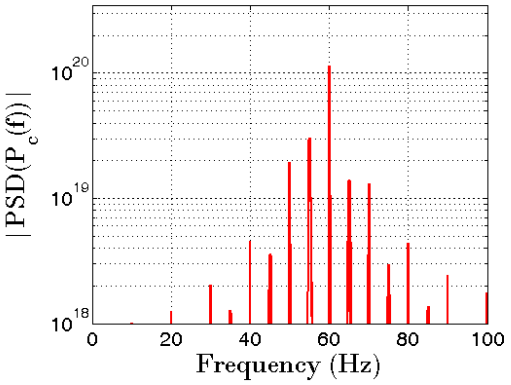

(b) $\Delta p_{ox}/p_c = 0.4$

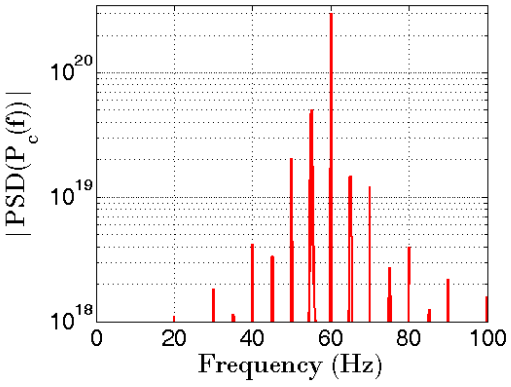

(c) $\Delta p_{ox}/p_c = 0.35$

Figure 5: Double time lag, $\Delta p_{fu}/p_c$ = 0.5: Power Spectral Density at different oxidizer injector pressure drops

For the constant time lag model we finally investigate the influence of different input amplitudes for various fuel pressure drops. The scope is here to investigate how the stability boundaries are influenced by the level of the input perturbations. In particular, we present the results obtained when the amplitude ϵ in eq.(10) is increased of 20% and 100%. The results in terms of the RMS of chamber pressure oscillations are then normalised with those obtained with the reference

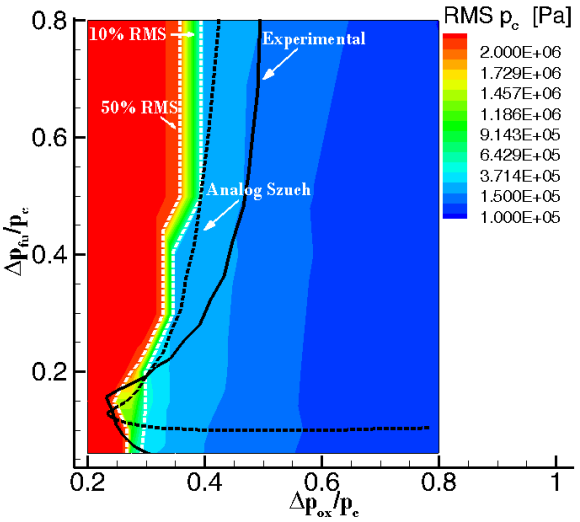

Figure 6: Stability map. Chamber pressure RMS dependency on oxidizer and fuel injector pressure drops

case $\epsilon = 0.01$ and then divided by the respective percentage increment. The aim of these normalisations is to investigate whether the response of the system is proportional to the input increment. Results shown in Fig. 7 highlight that for different fuel injector pressure drops the system response has a maximum at higher oxidizer injector pressure drops, thus evidencing that when the amplitude of the input perturbation is increased the boundary of the stability regions experience a greater shift if placed in the high pressure drop region and a smaller shift if placed in the low pressure drop region. Furthermore, increasing the input amplitude does not affect the characteristic frequency of the system that remains equal to 60 Hz.

4.1.2 Variable Time Lag

The time lags are typically not known a priori, hence when a new engine configuration is analysed it is useful to retrieve the needed time delays by means of dedicated correlations. The benefit of introducing correlations for the time lags is dual: on one hand the user is free from any a priori calculation of the time lags and, on the other hand, the time lags become time varying functions eq.(10) of the combustion chamber variables. In this frame we introduced semi-empirical correlations to calculate atomisation and vaporisation time lags, considering the combustion as infinitely fast. As previously mentioned the time lags for atomisation and vaporisation processes are retrieved respectively from eq.(6) and eq.(4), while mixing time lag is evaluated from an empirical curve [12]. A double time lag approach is still used, hence the total time delay for the liquid oxygen is retrieved as the sum of vaporisation, atomisation and mixing time lags while only the mixing time lag characterises the gaseous hydrogen delay. Some

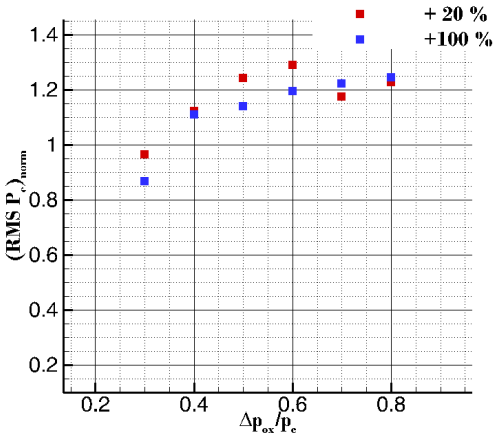

(a) $\Delta p_{fu}/p_c = 0.1$

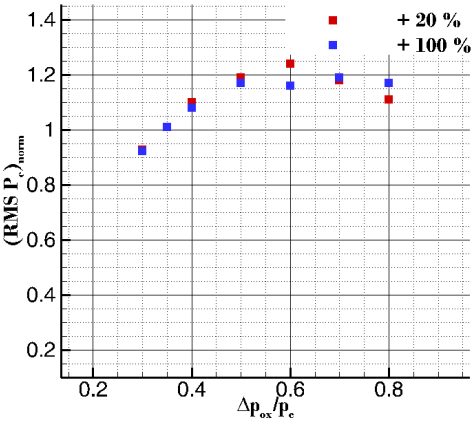

(b) $\Delta p_{fu}/p_c = 0.15$

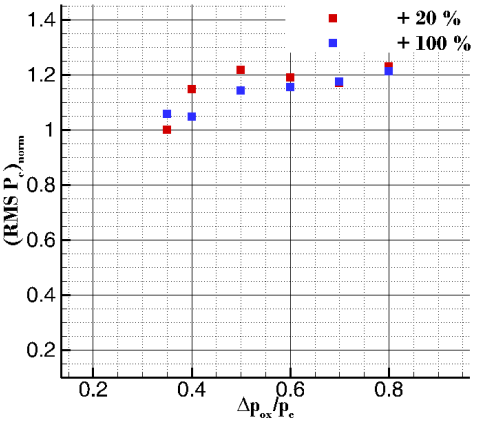

(c) $\Delta p_{fu}/p_c = 0.4$

Figure 7: Double time lag: normalised RMS of the chamber pressure signal for different input amplitudes at various fuel injector pressure drops

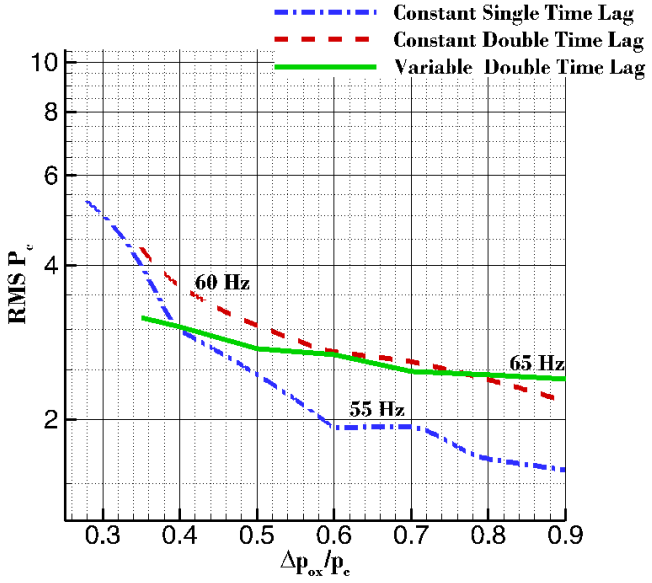

Figure 8: Double time lag, $\Delta p_{fu}/p_c = 0.5$: Chamber pressure RMS vs oxidizer injector pressure drops

considerations must be done on the correlation for the initial droplet diameter eq.(9). Due to the lack of informations on the experimental set up, the recess of the oxidizer post R_{post} is an unknown data that greatly influences the value of the initial droplet diameter and in turn the vaporisation time. Furthermore, the injector coefficient C_{inj} can range from 0.4 to 1.2, thus changing significantly the vaporisation delay. We know, from experimental evidences [27], that the initial droplet diameters of liquid oxygen at high pressure range from 60 μm to 160 μm. Hence, stated that the recess length is a construction parameter of a few millimetres, we decided to use a combination of values that, while respecting all of the aforementioned constraints, ensures a vaporisation time lag at steady state equal to $\tau_{vap} = 4.4$ ms. In this way we retrieved a time varying time lag matching with the steady state values suggested from the experimental evidences [21]. The chosen reference working point is characterised by the values $R_{post} = 0.003$ m, $C_{inj} = 0.4$ and $K = 0.121$, see eq. (9).

The time dependent approach is then tested on the engine configuration characterised by the parameters in Table 1. A single fuel injector pressure drop is here investigated at different oxidizer injector pressure drops, and results are compared in Fig. 8 against those obtained for the constant time lag approaches. The variable time lag approach gives a pressure response in line with the fixed time lag approaches. The amplitudes of the oscillations are less influenced by the reduction of the the oxidizer injector pressure drop and a smoother growth is observed while passing from high to low injector pressure drops. Finally, the time dependent time lags give a characteristic frequency of 65 Hz approaching the experimental measured value of 66 Hz, with an uncertainty of 5 Hz re-

lated to the broadband sampling frequency. Furthermore, the tendency of the double time lag approach in anticipating the insurgence of the inherent stability limit is here confirmed. In fact, in both double time lag approaches the limit moves towards higher oxidizer pressure drops and for pressure drops lower than $\Delta p_{ox}/p_c = 0.35$ the system is not able to damp the imposed perturbation, causing the chamber pressure to diverge with a frequency equal to the characteristic frequency of 65 Hz.

4.2 Combustion Chamber and Feed Lines

To study the influence of the feed lines on the combustion chamber dynamics, we connect two pipes to the combustion chamber configuration already discussed and investigate the response of the new system. The system is depicted in Fig. 9, where the fuel and oxidizer lines are indicated respectively with the names *GH2_ line* and *LOX_ line*, while the upstream junction resistive components *jun_ in_ GH2* and *jun_ in_ LOX* are included to connect the capacitive boundary conditions to the capacitive pipe components. Being the lines not included in the reference experimental setup, we impose arbitrary values of pipe diameters of $D_{ox} = 3$ mm and $D_{fu} = 5$ mm respectively for liquid oxygen and gaseous hydrogen line. All the tests are performed with the constant time lag approach, retaining the time lag values of $\tau_{ox} = 6.6$ ms and $\tau_{fu} = 2.2$ ms. We first investigate the response of the system to a broadband input characterised by the values $f_0 = 0$ Hz, $\Delta f = 5$ Hz,$N = 20$ and $\epsilon = 0.01$, with reference to eq.(10). During the analysis the fuel injector pressure drop is constant and equal to $\Delta p_{fu}/p_c$ = 0.4 while the oxidizer injector pressure drop is varied. The RMS of the oscillations of the measured chamber pressure signal is reported in terms of percentage values with respect to the mean chamber pressure and compared to the case without feed lines. Results in Fig. 10 show

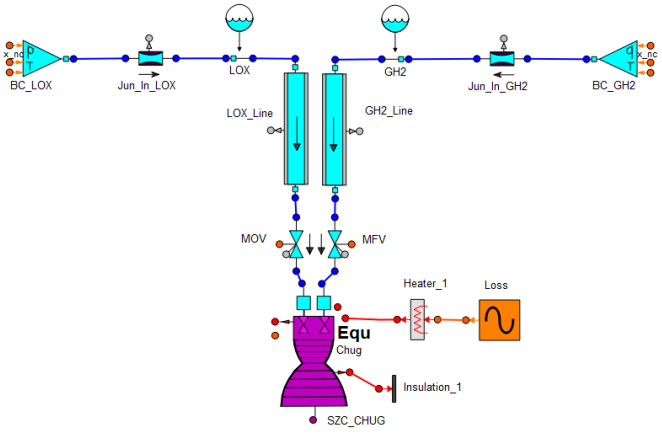

Figure 9: System schematic for chug analysis: combustion chamber with feed lines

that the feed lines have a stabilizing effect on the engine, and no unstable region is identified even at very low oxidizer pressure drops. The characteristics frequency is lowered to 45 Hz and overall response of the system is one order of magnitude smaller than the case in which the feed lines were not included. The stabilizing effect of the feed lines is hence confirmed [13]. Furthermore, even if not falling in an unstable regime the chamber pressure response still grows when the oxidizer injector pressure drop is reduced. To investigate the

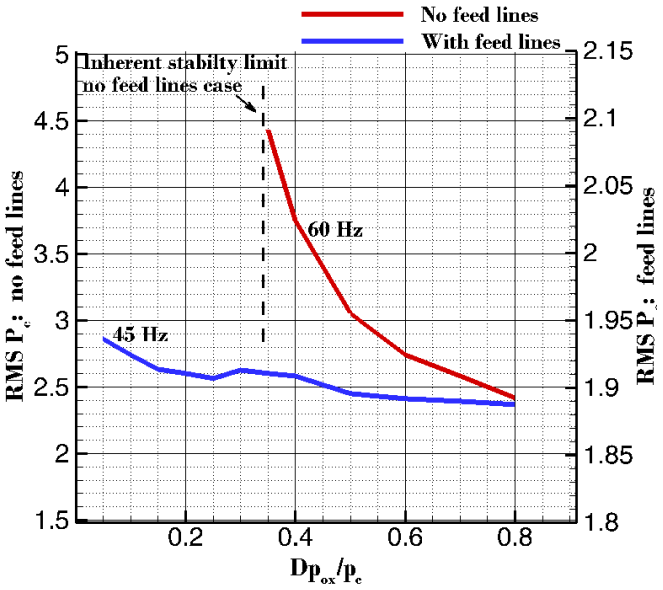

Figure 10: Double time lag, $\Delta p_{fu}/p_c$ = 0.4: Chamber pressure RMS vs oxidizer injector pressure drops

level of coupling between lines and combustion chamber we perform a series of test for a specific combination of injector pressure drops ($\Delta p_{ox}/p_c$ = 0.4, $\Delta p_{fu}/p_c$ = 0.4), varying the volume of the injector cavities. In the attempt of studying the influence of the feed lines on chug stability Wood et al. [31] noted that the effect of the dome compliance on the system was to drive the degree of the coupling between the combustion chamber and the upstream lines. The dome compliance is proportional to the dome volume that in our model is represented by the injector cavity components volume, hence to analyse this influence we vary the both cavity volumes and study the response of the system in terms of both pressure chamber RMS values and first characteristic frequencies. Once more the broad band input is characterised by the values $f_0 = 0$ Hz, $\Delta f = 5$ Hz,$N = 20$ and $\epsilon = 0.01$.

From Fig. 11 it can be pointed out that the decrease of the cavity volumes has a stabilizing effect on the system, and that a maximum in the system response is observed at intermediate values. As expected changing the volumes also the characteristic frequency of the system changes. In fact, as shown in Fig. 12, increasing the volumes the frequency goes from 45 Hz to 65 Hz passing through a maximum of about 90 Hz. Hence three distinct zones can be identified: (i) for small volumes the system is characterised by a small (and stable) response with a frequency of 45 Hz, (ii) for large volume values the feed lines are decoupled from the chamber, the response is higher and characterised by a frequency of 65 Hz as in the

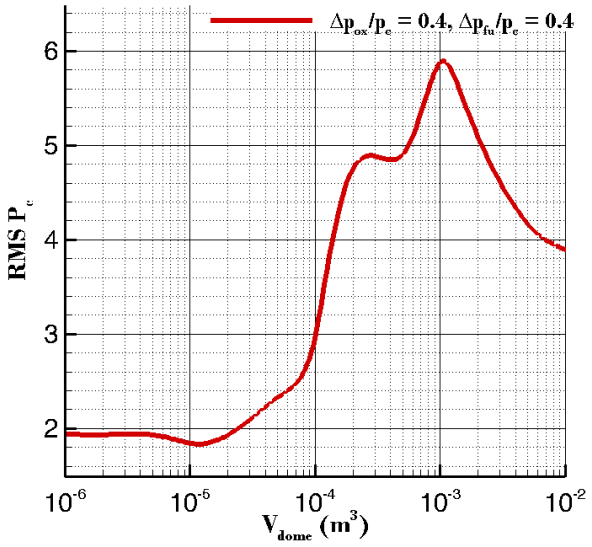

Figure 11: Double time lag, $\Delta p_{fu}/p_c = 0.4$, $\Delta p_{ox}/p_c = 0.4$: Chamber pressure RMS vs injector cavity volumes

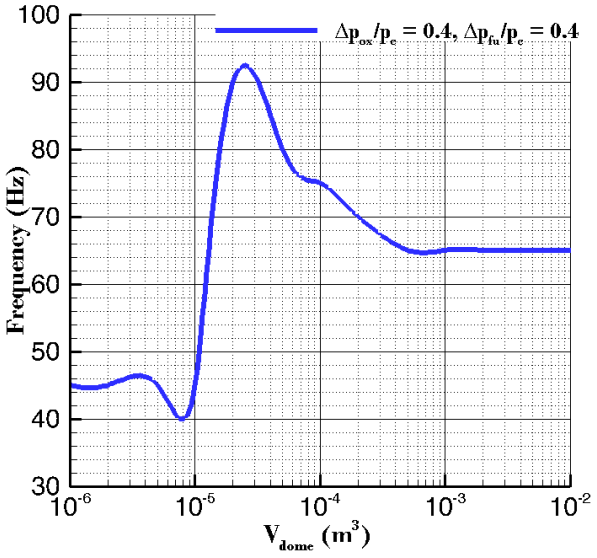

Figure 12: Double time lag, $\Delta p_{fu}/p_c = 0.4$, $\Delta p_{ox}/p_c = 0.4$: Chamber pressure frequency vs injector cavity volumes

case where no feed lines were considered and (iii) a transition zone where both response and characteristic values varies not monotonically with volume.

5 Conclusion

A double time lag model to investigate low frequency combustion instabilities has been implemented in the system analysis tool EcosimPro and tested against experimental results. Two different approaches have been followed: a constant time lag and a variable time lag approach based on semi-empirical correlations. The constant time lag approach demonstrates its effectiveness in reproducing the unstable behaviour associated with the reduction of the injector pressure drops, in particular no stable region has been identified for an oxidizer injector pressure drop lower than 0.35. The chug module is able to reproduce the reversal in slope of the stability boundary at low injector pressure drops, thus giving a result close to the one found in the reference experiment. However, it must be pointed out that the location of the stability boundary depends on both the criterion used to define the regime as unstable and on the amplitude of the input perturbation. We demonstrated that the boundaries can be easily shifted by changing the amplitude of the input perturbation and that this shift slightly depends on the selected injector pressure drop. Hence, in the computer program the stability boundaries can be shifted in accordance with the level of the input perturbation. Despite its simplicity, the constant time lag approach is able to predict a characteristic frequency close to the one measured experimentally. The high frequency content is characterised by a ratio of higher to lower frequency close to 2.7, as reported in open literature. It must be noted that in our case the high frequency does not dominate the dynamic response at low fuel injector pressure drops and the instability is still related to the first characteristic frequency. The inability in catching the suppression of the first mode could be related with a lack of data for parameters that usually influence the damping effect and the associated system impedances, i.e. injector cavity volumes and length of the feed lines. These values have been selected to be consistent with the downstream injector geometry and mass flow rates, but a fine tuning with the real data is unavoidable to improve the results of the model. The chug module has been finally tested with semi-empirical correlations to retrieve characteristic delays that, depending on the main flow variables, are time dependent functions of the main combustion chamber parameters. With the implemented correlations the model retrieves a lower characteristic frequency that better approximates the experimental results, while the predicted RMS values of the chamber pressure remain comparable with those obtained with the constant double time lag model. Finally, the study on the influence of the feed lines confirmed the stabilising effect of the system on the combustion chamber. As expected, the stabilisation appears to be strictly related to the dome volumes, since increasing the volumes upstream the combustion chamber cause the decoupling of the chamber from the rest of the system and progressively reduces the influence of the lines on the combustion chamber dynamics.

Acknowledgements

The work in this paper was conducted in the frame of the Network Partnering Initiative agreement between the European Space Agency (ESA) and the Dipartimento di Ingegneria Meccanica e Aerospaziale (DIMA) of 'La Sapienza' Univer-

sity of Rome.

REFERENCES

[1] Casiano, M. J., *Extensions to the Time Lag Models for Practical Application to Rocket Engine Stability Design*, Ph.D. thesis, The Pennsylvania State University, 2010.

[2] Summerfield, M., "A theory of unstable combustion in liquid propellant rocket systems," *Journal of the American Rocket Society*, Vol. 21, No. 5, 1951, pp. 108–114.

[3] Gunder, D. and Friant, D., "Stability of flow in a rocket motor," *Journal of applied mechanics- Transactions fo the ASME*, Vol. 17, No. 3, 1950, pp. 327–333.

[4] Wenzel, L. M. and Szuch, J. R., *Analysis of Chugging in Liquid-Bipropellant Rocket Engines Using Propellants with Different Vaporization Rates*, National Aeronautics and Space Administration, 1965.

[5] Crocco, L., "Aspects of combustion stability in liquid propellant rocket motors part I: fundamentals. Low frequency instability with monopropellants," *Journal of the American Rocket Society*, Vol. 21, No. 6, 1951, pp. 163–178.

[6] Webber, W., "Calculation of low-frequency unsteady behavior of liquid rockets from droplet combustion parameters," *Journal of Spacecraft and Rockets*, Vol. 9, No. 4, 1972, pp. 231–237.

[7] Bartrand, T. A., *A study of low frequency combustion instability in rocket engine preburners using a heterogeneous stirred tank reactor model*, Ph.D. thesis, University of Tennessee, Knoxville, 1987.

[8] Empresarios Agrupados, "EcosimPro: Continuous and Discrete Modelling Simulation Software," http://www.ecosimpro.com, 2007.

[9] Empresarios Agrupados, "ESPSS User Manual," 2.4 edition, 2012.

[10] Crocco, L., "Aspects of Combustion Stability in Liquid Propellant Rocket Motors Part II: Low Frequency Instability with Bipropellants. High Frequency Instability," *Journal of the American Rocket Society*, Vol. 22, No. 1, 1952, pp. 7–16.

[11] Crocco, L. and Cheng, S.-I., *Theory of combustion instability in liquid propellant rocket motors*, Cambridge Univ Press, 1956.

[12] Szuch, J. R., *Digital computer program for analysis of chugging instabilities*, National Aeronautics and Space Administration, 1970.

[13] Harrje, D. T. and Reardon, F. H., "Liquid propellant rocket combustion instability," *NASA Special Publication*, Vol. 194, 1972.

[14] Szuch, J. R., "Application of a double-dead-time model describing chugging to liquid propellant rocket engines having multielement injectors," Technical Note TN D-5303, NASA, 1969.

[15] Ordonneau, G., Girard, N., and David, N., "Analysis and modeling of Vulcain engine shutdown transient chugging," *Office National d'etudes et de recherches aerospatiales ONERA-PUBLICATIONS-TP*, , No. 143, 2000.

[16] Ordonneau, G., Levy, F., and Girard, N., "Low frequency oscillation phenomena during VULCAIN shutdown transient," *AIAA/ASME/SAE/ASEE Joint Propulsion Conference and Exhibit, 37 th, Salt Lake City, UT*, 2001.

[17] Fang, J., "Application of combustion time-lag theory to combustion stability analysis of liquid and gaseous propellant rocket engines," *AIAA 22nd Aerospace Sciences Meeting*, January 9-12,Reno,Nevada 1984.

[18] Sirignano, W. A., Deplanque, J., Chiang, C., and Bhatia, R., "Liquid-Propellant Droplet Vaporization: A Rate-Controlling Process for Combustion Instability," *Liquid Rocket Engine Combustion Instability*, Progress in Astronautics and Aeronautics 1995, pp. 307–343.

[19] Boronine, E., Vollmer, K., and Frey, M., "A modified ESPSS combustion chamber model with chugging modeling capability," ESPSS 2^{nd} Workshop, ESTEC, Noordwijk, The Nederlands.

[20] Vingert, L., Gicquel, P., Ledoux, M., Carré, I., Micci, M., and Glogowski, M., "Atomization in Coaxial-Jet Injectors," *Progress in Astronautics and Aeronautics*, Vol. 200, 2004, pp. 105–140.

[21] Szuch, J. R. and Wenzel, L. M., "Experimental verification of a double-dead-time model describing chugging in liquid-bipropellant rocket engines." Tech. rep., NASA, 1967.

[22] Di Matteo, F., *Modelling and Simulations of Liquid Rocket Engine Ignition Transients*, Ph.D. thesis, University of Rome "La Sapienza", 2012.

[23] Bruce Stewart, H. and Wendroff, B., "Two-phase flow: models and methods," *Journal of Computational Physics*, Vol. 56, No. 3, 1984, pp. 363–409.

[24] Meng, H., Hsiao, G., Yang, V., and Shuen, J., "Transport and dynamics of liquid oxygen droplets in supercritical hydrogen streams," *Journal of Fluid Mechanics*, Vol. 527, 2005, pp. 115–139.

[25] Ranz, W. and Marshall, W., "Evaporation from drops," *Chemical Engineering Progress*, Vol. 48, No. 3, 1952, pp. 141–146.

[26] Yang, V., "Liquid-Propellant Droplet Combustion and Cluster-Behavior at Supercritical Conditions," Tech. rep., DTIC Document, 2001.

[27] Lafon, P., Meng, H., Yang, V., and Habiballah, M., "Vaporization of liquid oxygen (LOX) droplets in hydrogen and water environments under sub-and supercritical conditions," *Combustion Science and Technology*, Vol. 180, No. 1, 2007, pp. 1–26.

[28] Ferrenberg, A. and Varma, M., "Atomization data requirements for rocket combustor modeling," *APL 21st JANNAF Combust. Meeting*, Vol. 1, 1984, pp. 369–377.

[29] Priem, R. and Heidmann, M., *Propellant vaporization as a design criterion for rocket-engine combustion chambers*, Vol. 67, National Aeronautics and Space Administration, 1960.

[30] Anon, "J-2 Program Quarterly Progress Report for Period Ending February 28, 1962," Tech. Rep. Rep.No. R-2600-6(NASA CR-63323), Rocketdyne Div., pp.85, 137-140, Mar. 28 1962, North American Aviation.

[31] Wood, D. and Dorsch, R., "Effect of propellant-feed-system coupling and hydraulic parameters on analysis of chugging," Technical Note TN D-3896, NASA, 1967.